Supplementary Materials

For

Novel crosslinker for synthesizing hypercrosslinked ionic polymers containing activating groups as efficient catalysts for CO_2 cycloaddition reaction

Xu Liao[a], Xiaoyan Xiang[a], Zeyu Wang[a], Ruixun Ma[b], Lingzheng Kong[b], Xilin Gao[a], Jiao He[a], Wenjuan Hou[c], Cheng Peng [a,*], Jinqing Lin[a,*]

[a] *College of Materials Science and Engineering, Huaqiao University, Xiamen 361021, China*

[b] *College of Chemical Engineering, Huaqiao University, Xiamen 361021, China*

[c] *Instrumental Analysis Center, Huaqiao University, Xiamen 361021, China*

E-mail: chengpeng@hqu.edu.cn (Cheng Peng); linlab@hqu.edu.cn (Jingqin Lin).

Supplementary Experimental

1.1 Materials

The commercial chemicals and reagents were used as received without further purification unless otherwis stated. 4,4'-bis(chloromethyl)-1,1'-biphenyl (BCB, 96%), 4,4'-bis(bromomethyl)biphenyl (BBB, 97%), bromoacetaldehyde dimethyl acetal (BDC, 97%), 1,2-dichloroethane (DCE, AR), 2, 2-chloro-1,1-dimethoxyethane (CDA, 98%), dimethoxymethane (FDA, 98%), anhydrous ferric chloride ($FeCl_3$, AR), 1-methyl-1H-imidazole-2-carboxylic acid (90%), epichlorohydrin (AR), allyl glycidyl ether (99%), butyl glycidyl ether (98%) were provided by Aladdin Chemical Reagent Co. LTD. 1H-imidazole-2-methanol (98%), 1,2-dimethylimidazole (98%), styrene oxide (98%), glycidyl phenyl ether (99%), epibromohydrin (98%), dibromomethane (98%) were purchased from Energy Chemical Reagent Co.LTD. O-tolyl glycidyl were provided by Macklin Chemical Reagent Co. LTD.

1.2 Characterization

The IR spectra were characterized by using an FT-IR (3500~500 cm^{-1}) spectrometer at 4 cm^{-1} resolution and 32 scans (Nicolet Nexus FT-IR spectrometer, USA). NMR spectra were obtained in $CDCl_3$ on a Bruker AVANCE III 500MHz spectrometer for ^1H NMR, the particular NMR spectra can be found in the supplementary information. ^{13}C CP/MAS NMR spectra were measured on an Agilent-NMR-vnmrs 600. Thermogravimetric analysis of the samples were heated from 50 °C to 800 °C at ramp 10 °C/min Under Ar (TGA-50H, Shimadzu). Brunauer-Emmett-Teller (BET) pore volumes and surface areas were calculated at 77 K by using JWGB (JW-DEL 200), CO_2 sorption isotherms were recorded at 273 K and 298 K. The crystal structure of the samples were examined by X-ray diffraction (XRD) on SmartLa. CHNS elemental analysis were performed on Vario EL Cube.

Field emission scanning electron microscope (FESEM; Hitachi S-4800, accelerated voltage: 5 kV) was used to observe the morphology. Transmission electron microscope (TEM) images of the samples were obtained by Hitachi H-7650. X-ray photoelectron spectroscopy (XPS) of the HIP(3)-OH was determined by Thermo Fisher Scientific K-alpha^{+} equipped with Al K radiation (1486.68 eV).

1.3 Synthesis of polymers

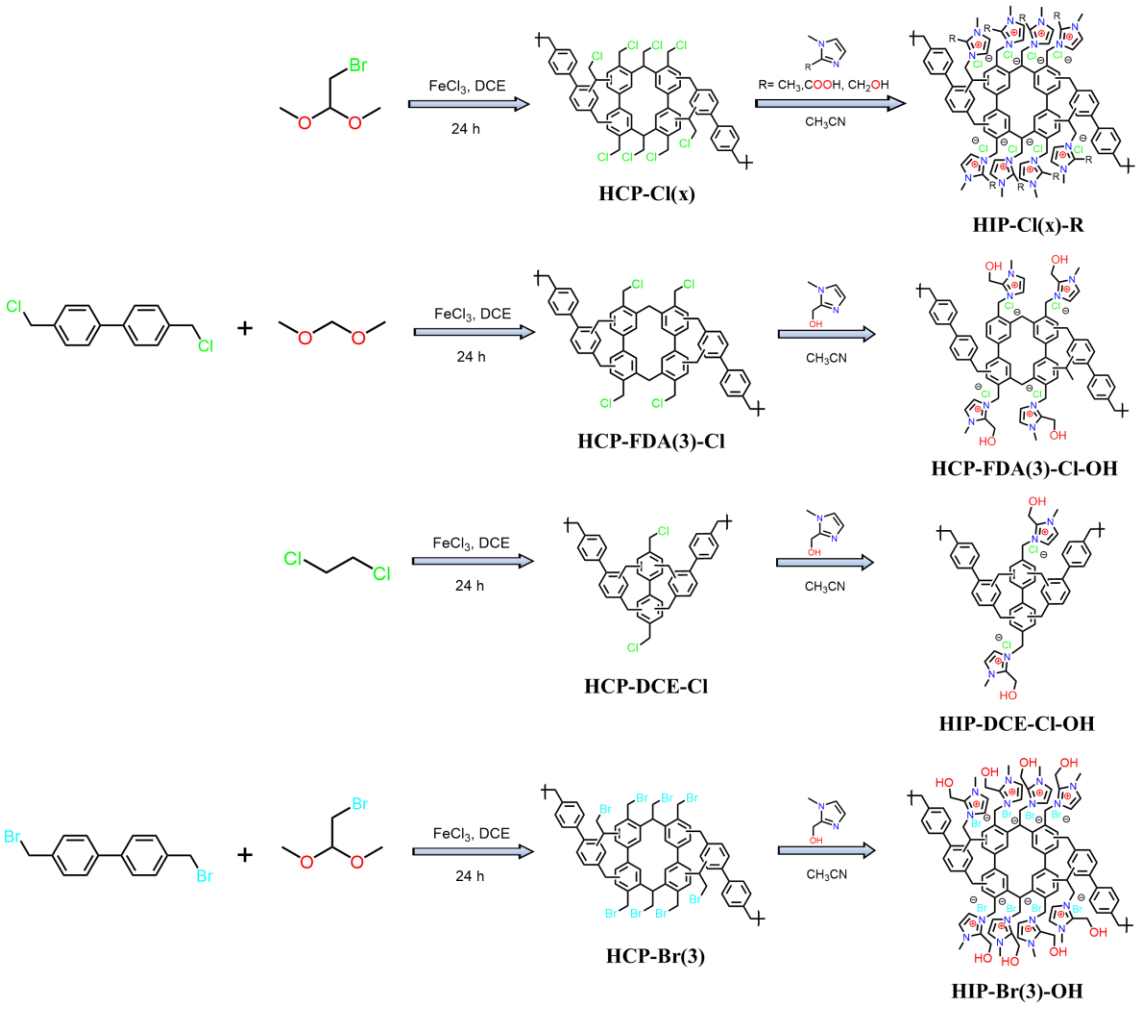

Scheme S1. Synthesis of HIPs.

Supplementary Figures

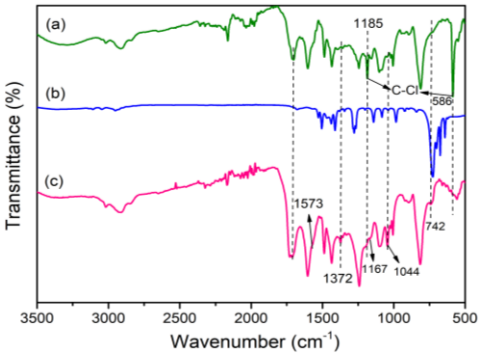

Fig. S1. (a) HCP-Cl(3), (b) 1,2-Dimethylimidazole, (c) HIP-Cl(3)-CH_3.

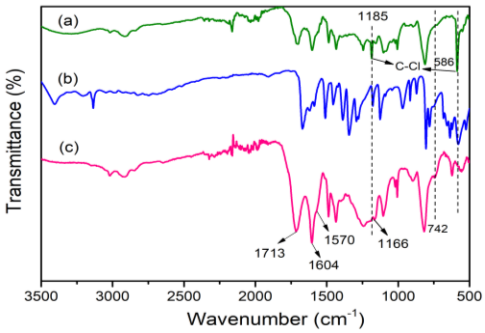

Fig. S2. (a) HCP-Cl(3), (b) 1-Methyl-1H-imidazole-2-carboxylic acid, (c) HIP-Cl(3)-COOH.

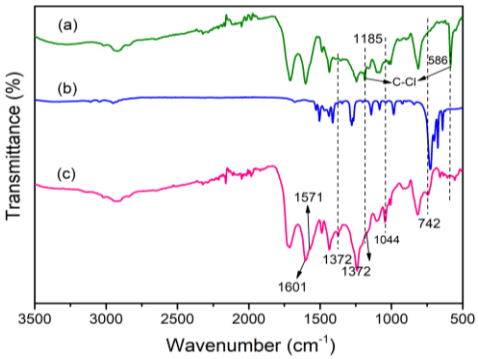

Fig. S3. (a) HCP-Cl(5), (b) 1,2-Dimethylimidazole (c) HIP-Cl(5)-CH_3.

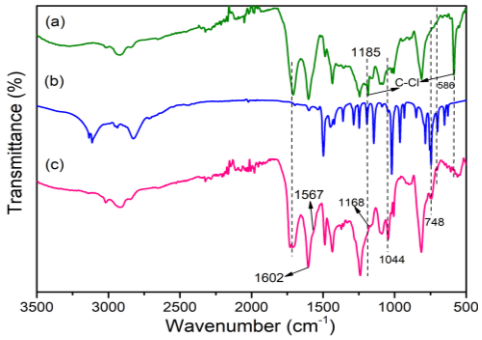

Fig. S4. (a) HCP-Cl(5), (b) 1H-Imidazole-2-methanol (c) HIP-Cl(5)-OH.

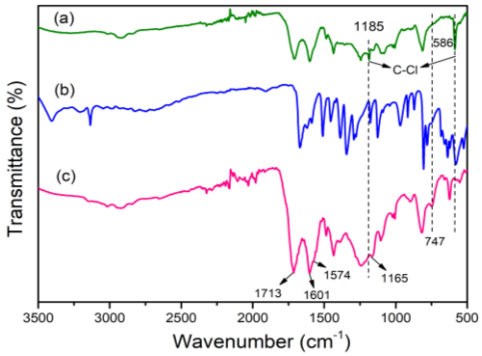

Fig. S5. (a) HCP(5)-Cl, (b) 1-Methyl-1H-imidazole-2-carboxylic acid, (c) HIP(5)-COOH.

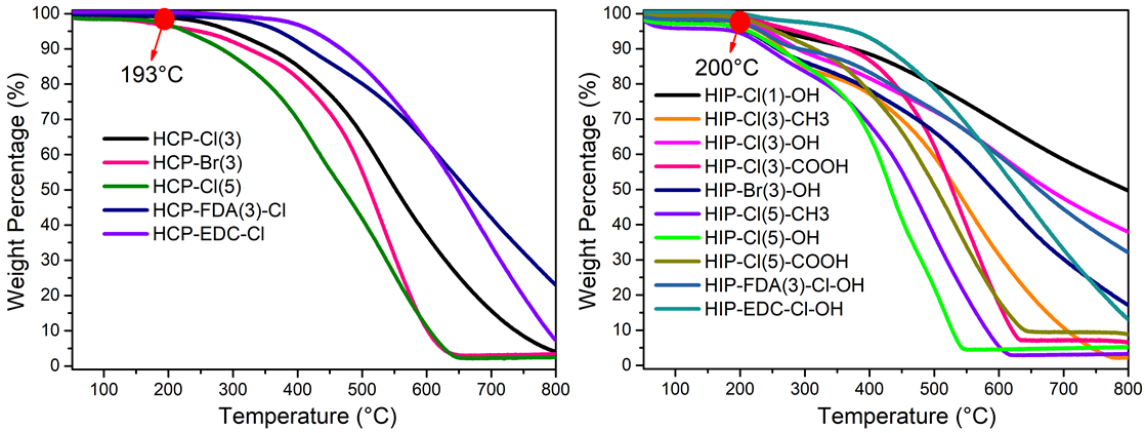

Fig. S6. TG curve of HCPs and HIPs.

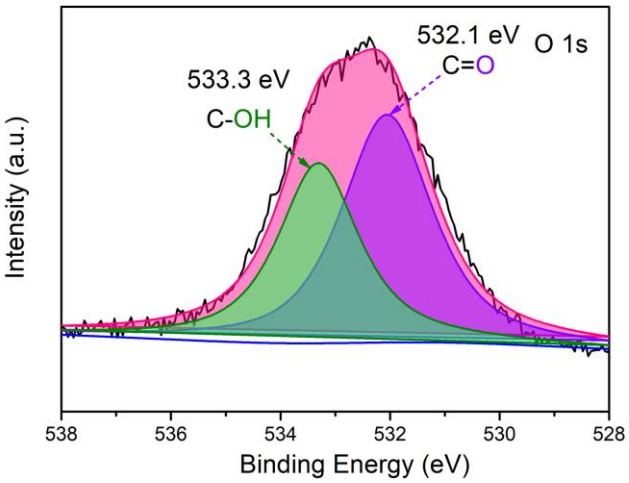

Fig. S7. O 1s XPS spectra of HIP-Cl(3)-OH.

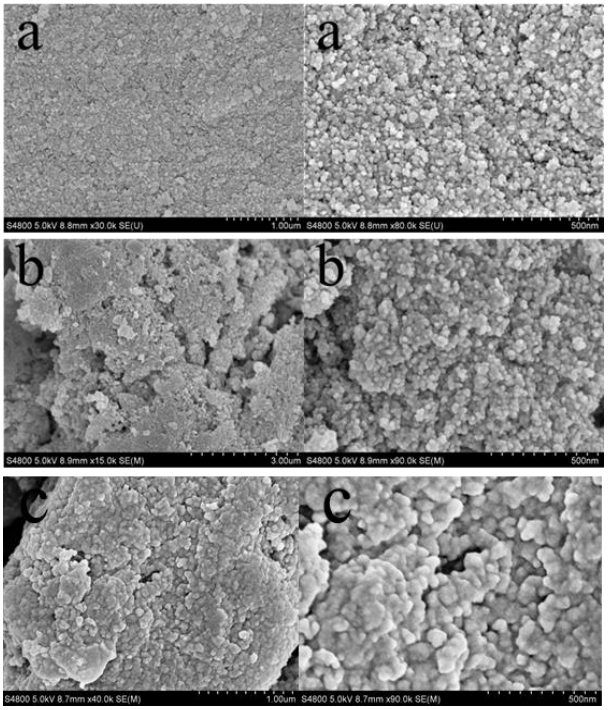

Fig. S8. SEM images of (a) HCP-Cl(3), (b) HIP-Cl(3)-OH, (c) HIP-Cl(3)-OH after run 6 th.

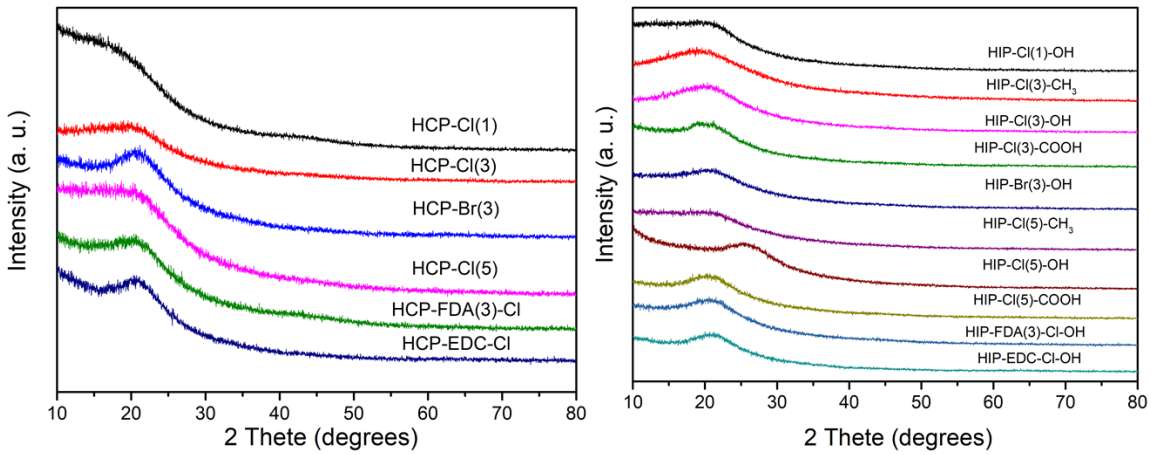

Fig. S9. XRD patterns of HCPs and HIPs.

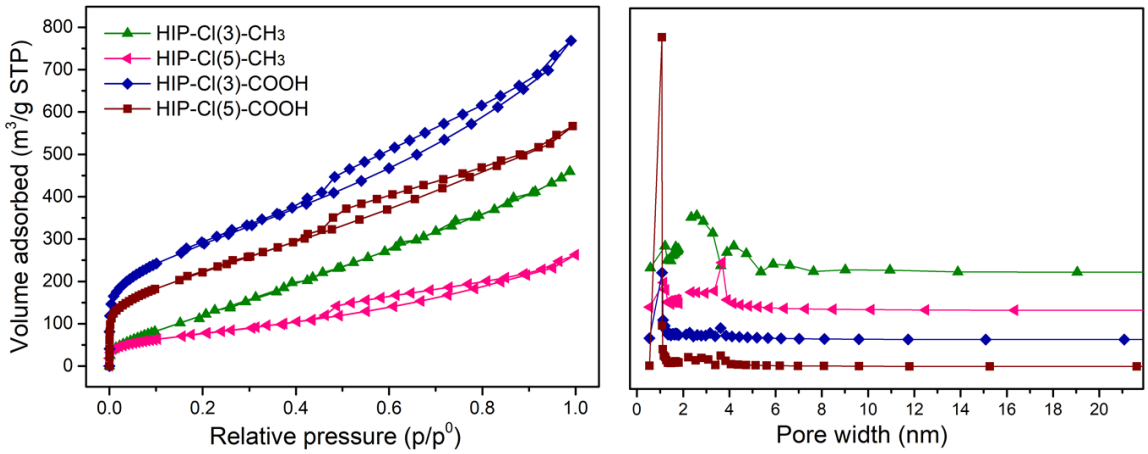

Fig. S10. (a) N_2 sorption isotherm and (b) pore size distribution curve of HIP-Cl(3)-CH_3, HIP-Cl(3)-COOH, HIP-Cl(5)-CH_3, HIP-Cl(5)-COOH.

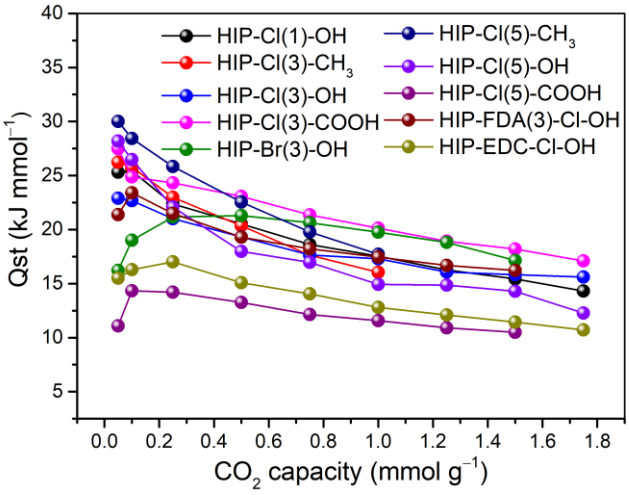

Fig. S11. The isosteric heats of adsorption, as calculated from the adsorption curves at two different temperatures 273K and 289K: HIP-Cl(1)-OH, HIP-Cl(3)-CH_3, HIP-Cl(3)-COOH, HIP-Cl(3)-OH, HIP-Br(3)-OH, HIP-Cl(5)-CH_3, HIP-Cl(5)-COOH, HIP-Cl(5)-OH, HIP-FDA(3)-Cl-OH, HIP-EDC-Cl-OH.

^{1}H NMR spectra of cyclic carbonates

Calculate the yield by using dibromomethane as a standard sample and significant peak is about 4.86 ppm, the peak of ethyl acetate is about 3.90, 1.84, 1.06 ppm.

Fig. S12 ^{1}HNMR spectra (in $CDCl_3$) of the reaction mixture using HIP-Cl(3)-OH as a catalyst for the cycloaddition reaction of Epichlorohydrin (*^{1}H NMR spectrum was obtained from the crude sample*). ^{1}H NMR (500 MHz, $CDCl_3$) δ: 4.90 (m, 1H), 4.45 (t, J=8.6 Hz, 1H), 4.23 (dd, J=3.0, 5.8 Hz, 1H), 3.71 (dd, J=4.1, 12.4 Hz, 1H), 3.61 (dd, J=3.7, 12.2 Hz, 1H).

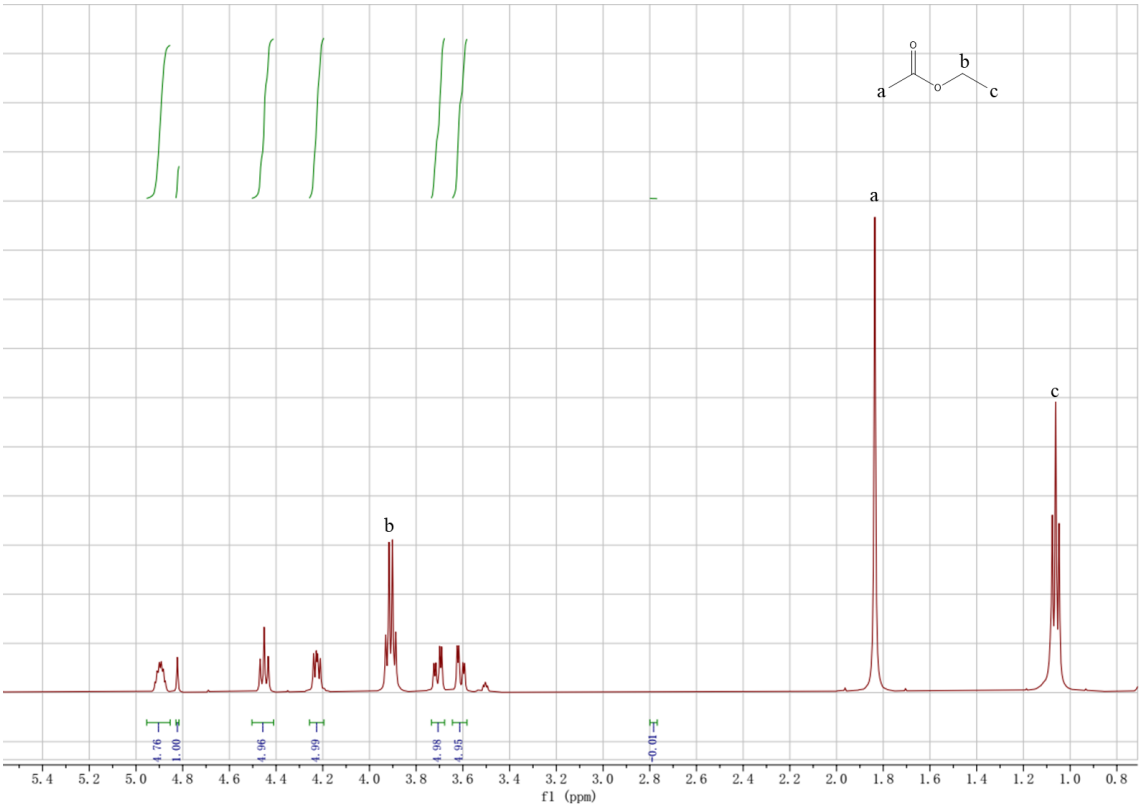

Fig. S13 ^{1}HNMR spectra (in $CDCl_3$) of the reaction mixture using HIP-Cl(3)-OH as a catalyst for the cycloaddition reaction of Epibromohydrin (*^{1}H NMR spectrum was obtained from the crude sample*). ^{1}H NMR (500 MHz, $CDCl_3$) δ: 4.94 (m, 1H), 4.54 (t, J=8.6 Hz, 1H), 4.28 (dd, J=3.0, 5.9 Hz, 1H), 3.59 (dd, J=5.4, 11.2 Hz, 1H), 3.61 (dd, J=3.9, 11.3 Hz, 1H).

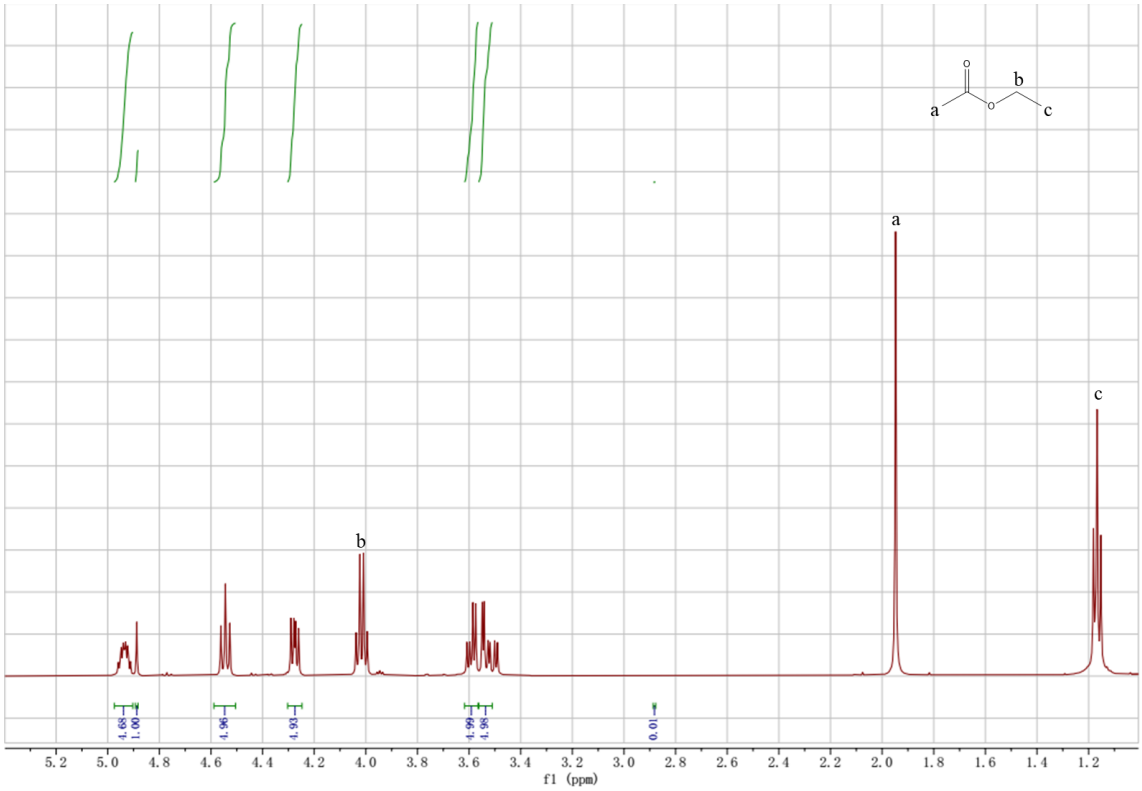

Fig. S14 ^{1}HNMR spectra (in $CDCl_3$) of the reaction mixture using HIP-Cl(3)-OH as a catalyst for the cycloaddition reaction of Styrene oxide (*^{1}H NMR spectrum was obtained from the crude sample*). ^{1}H NMR (500 MHz, $CDCl_3$) δ: 7.41-7.34 (m, Ar-H, 5H), 5.65 (t, J=8.1 Hz, 1H), 4.77 (t, J=8.5 Hz, 1H), 4.29 (t, J=8.0 Hz, 1H).

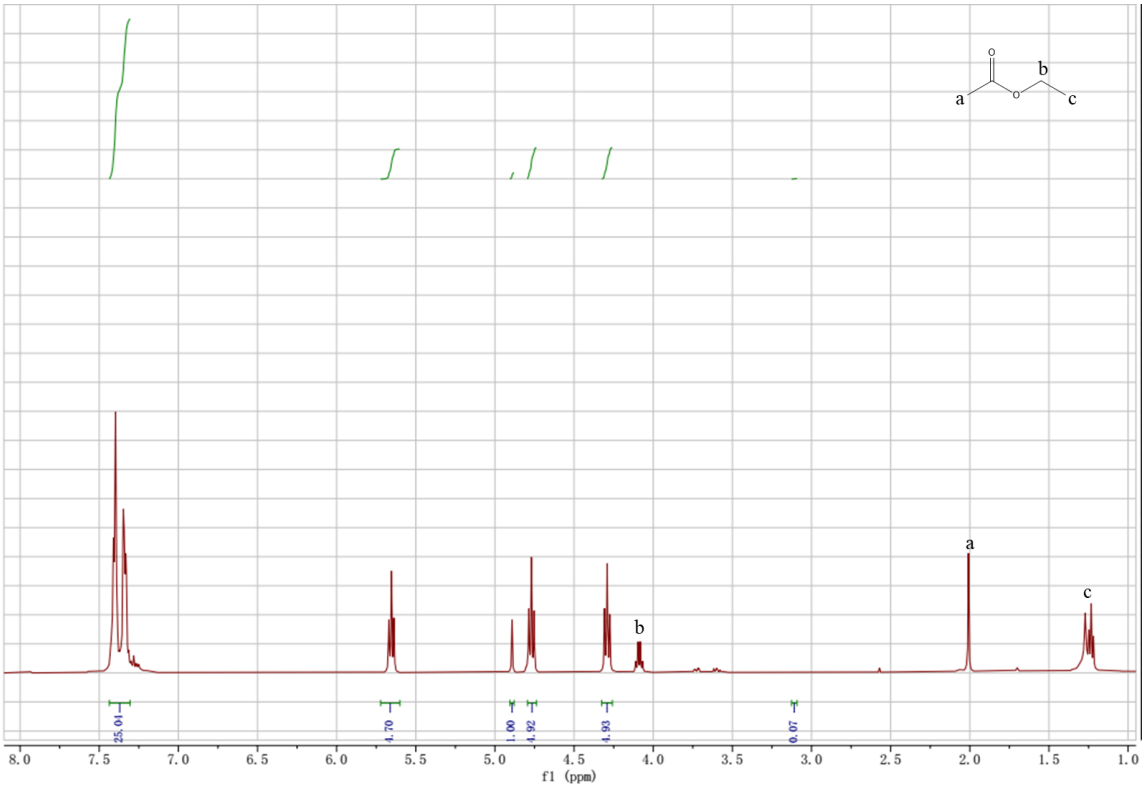

Fig. S15 ^{1}HNMR spectra (in $CDCl_3$) of the reaction mixture using HIP-Cl(3)-OH as a catalyst for the cycloaddition reaction of Glycidyl phenyl ether (*^{1}H NMR spectrum was obtained from the recrystallization)*. ^{1}H NMR (500 MHz, $CDCl_3$) δ: 7.33 (t, J=8.0 Hz, 2H), 7.04 (t, J=7.1 Hz, 1H), 6.94 (d, J =8.1 Hz, 2H), 5.05 (m, 1H), 4.64 (t, J=8.5 Hz, 1H), 4.56 (td, J=2.6, 5.9 Hz, 1H), 4.26 (dd, J=4.2, 10.5 Hz, 1H), 4.17 (dd, J=3.6, 10.6 Hz, 1H).

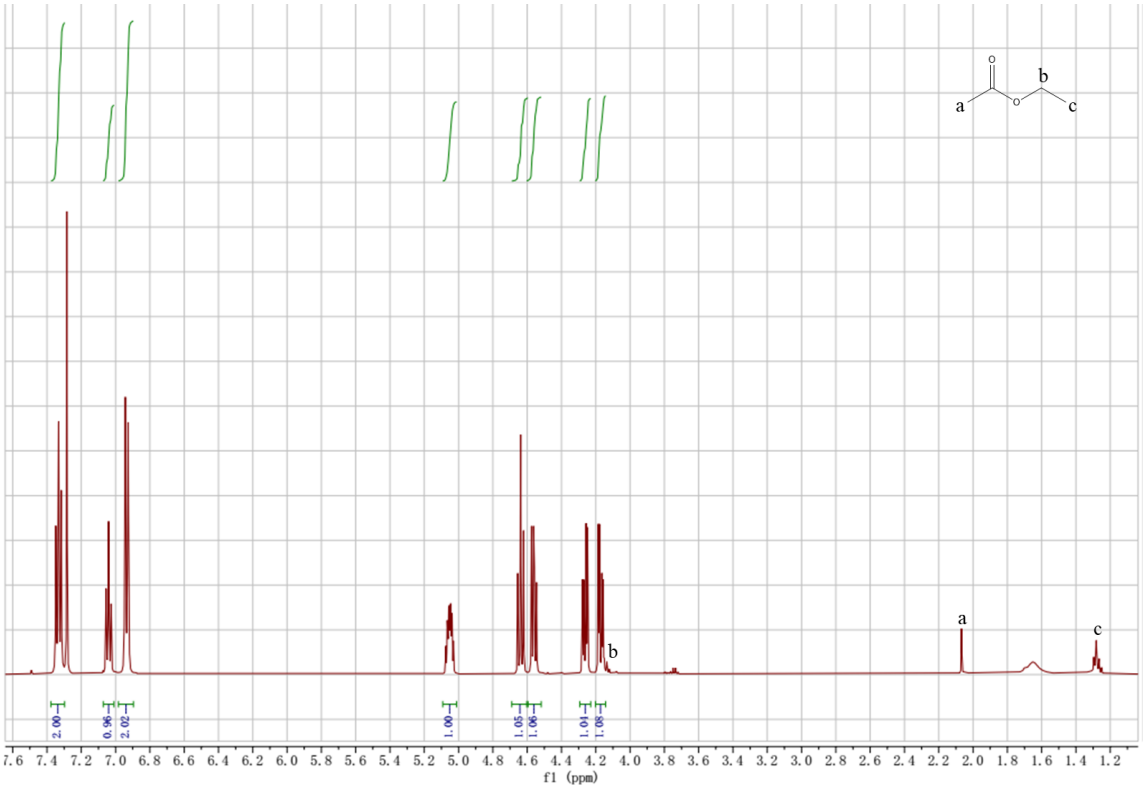

Fig. S16 ^{1}H NMR spectra (in $CDCl_3$) of the reaction mixture using HIP-Cl(3)-OH as a catalyst for the cycloaddition reaction of O-Tolyl glycidyl ether (*^{1}H NMR spectrum was obtained from the crude sample)*. ^{1}H NMR (500 MHz, $CDCl_3$) δ: 7.06 (t, J=7.4 Hz, 2H), 6.82 (t, J=7.2 Hz, 1H), 6.70 (d, J =8.4 Hz, 1H), 4.95 (m, 1H), 4.50 (t, J=8.5 Hz, 1H), 4.44 (td, J=3.1, 6.7 Hz, 1H), 4.13 (dd, J=2.9, 10.8 Hz, 1H), 3.99 (dd, J=3.2, 10.7 Hz, 1H), 2.13 (s, 3H).

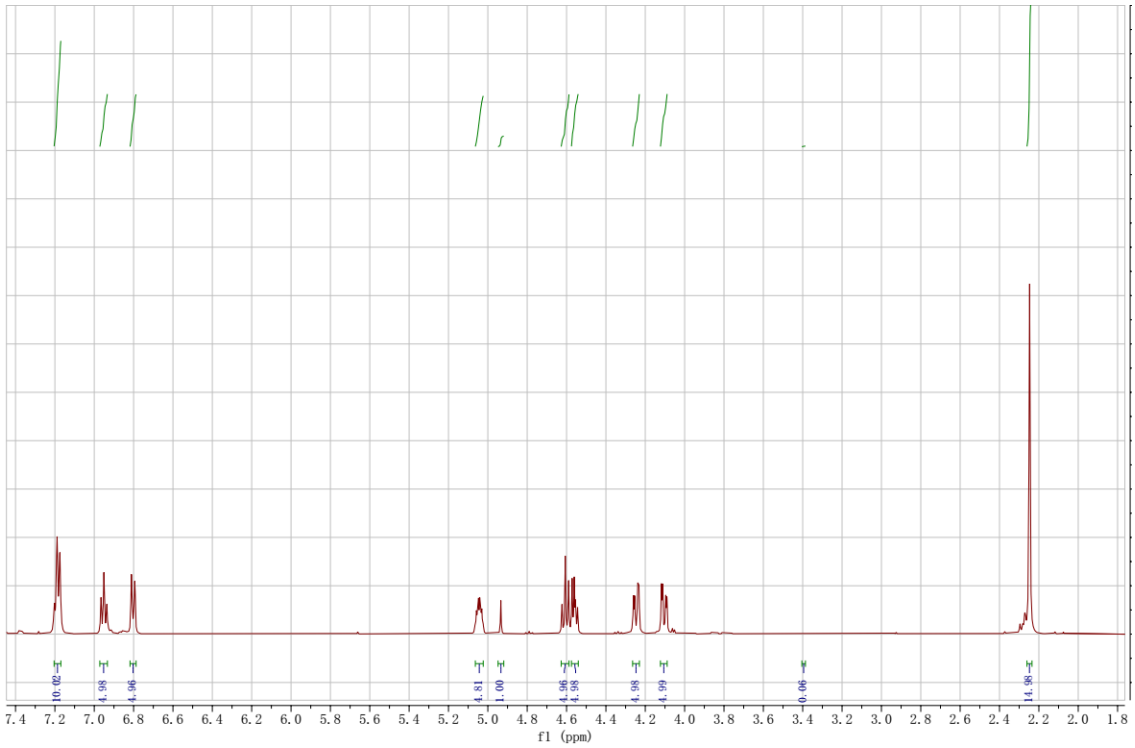

Fig. S17 ^{1}HNMR spectra (in $CDCl_3$) of the reaction mixture using HIP-Cl(3)-OH as a catalyst for the cycloaddition reaction of Allyl glycidyl ether (*^{1}H NMR spectrum was obtained from the crude sample*). ^{1}H NMR (500 MHz, $CDCl_3$) δ: 5.74 (m, 1H), 5.15 (dd, J=1.2, 17.3 Hz, 1H), 5.08 (d, J=10.4 Hz, 1H), 4.74 (m, 1H), 4.40 (t, J=8.2 Hz, 1H), 4.26 (dd, J=2.2, 6.1 Hz, 1H), 3.92 (d, J=5.6 Hz, 2 H), 3.46−3.36 (m, the product of allyl glycidyl ether obtained by free radical polymerization), 3.58 (dd, J=3.2, 11.2 Hz, 1H), 3.50 (m, 3H).

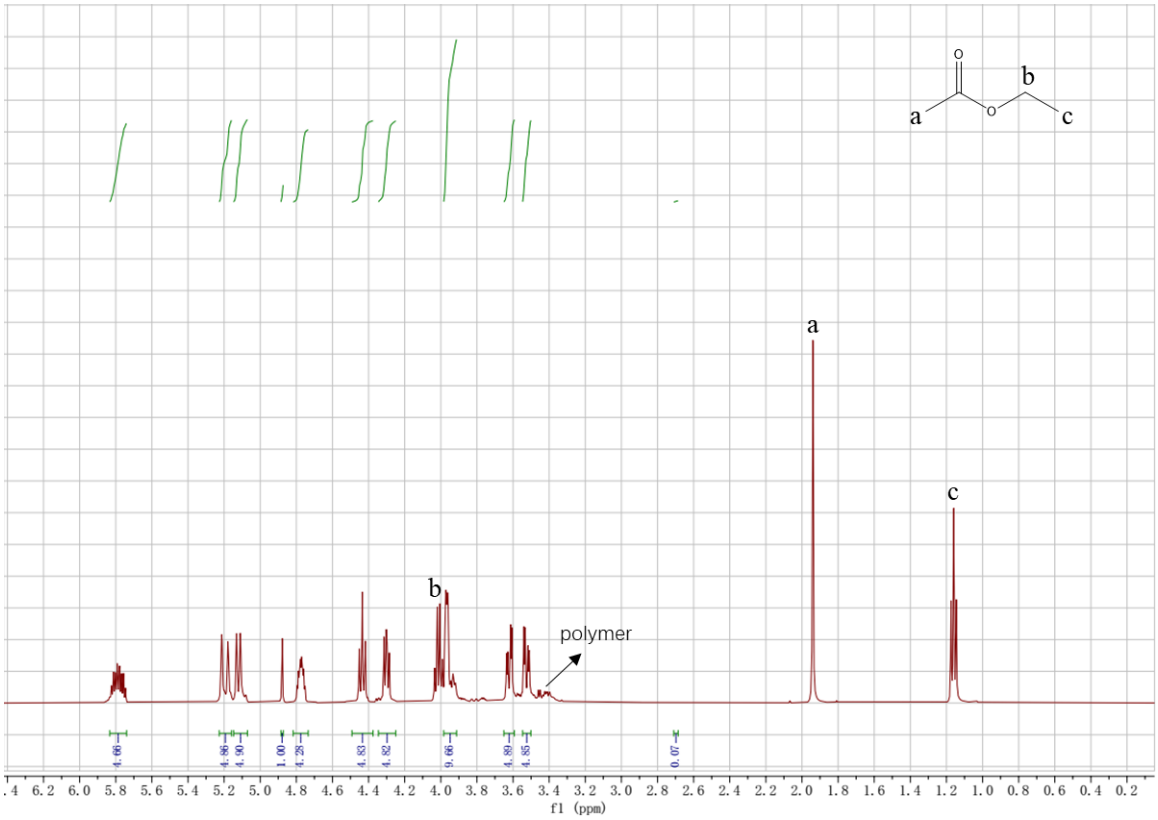

Fig. S18 ^{1}HNMR spectra (in $CDCl_3$) of the reaction mixture using HIP-Cl(3)-OH as a catalyst for the cycloaddition reaction of Butyl glycidyl ether (*^{1}H NMR spectrum was obtained from the crude sample*). ^{1}H NMR (500 MHz, $CDCl_3$) δ: 4.73 (m, 1H), 4.39 (t, J=8.5, 1H), 4.25 (dd, J=2.2, 5.9 Hz, 1H), 3.57 (dd, J=3.5, 11.2 Hz, 1H), 3.47 (dd, J=3.6, 11.2 Hz, 1H), 3.39 (dd, J=1.1, 6.6 Hz, 2H), 1.44 (m, 2H), 1.25 (m, 2H), 0.79 (t, J=7.4, 3H).

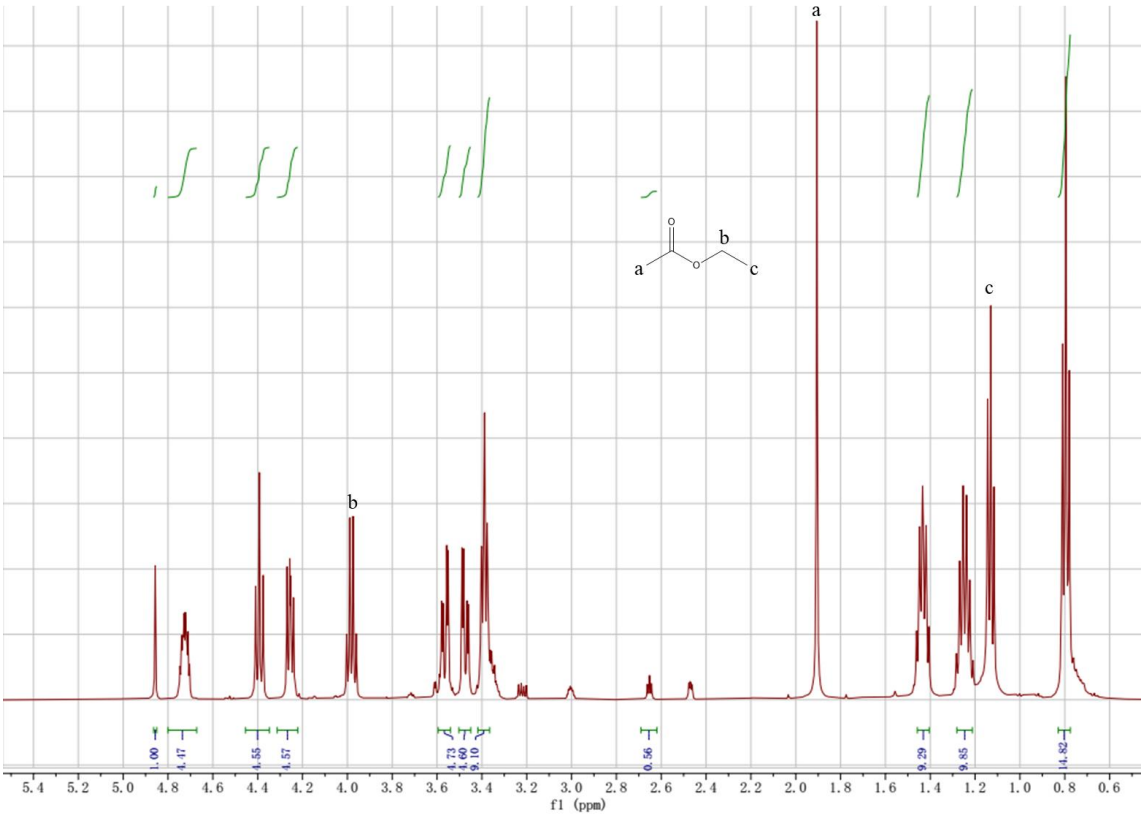

Table S1 Textual properties of HIPs.

Sample	S_{BET}[a] ($m^2 g^{-1}$)	V_p[b] ($cm^3 g^{-1}$)	V_{micro}[c] ($cm^3 g^{-1}$)	D_{total}[d] (nm)	D_{micro}[e] (nm)	CO_2 adsorption[f](mmol g^{-1})273K/298K	Qst (kJ mol^{-1})
HIP-Cl(1)-OH	976	0.894	0.570	3.665	1.076	2.73/1.82	25.23
HIP-Cl(3)-CH_3	374	0.793	0.101	8.483	1.681	1.63/1.09	26.23
HIP-Cl(3)-COOH	979	1.189	0.487	4.859	1.090	2.42/1.85	27.49
HIP-Cl(3)-OH	596	0.559	0.376	3.752	1.082	3.22/2.02	22.89
HIP-Br(3)-OH	537	0.670	0.276	4.985	1.095	2.11/1.49	16.23
HIP-Cl(5)-CH_3	255	0.407	0.100	6.361	1.154	1.54/1.01	30.01
HIP-Cl(5)-COOH	744	0.877	0.410	4.714	1.080	2.51/1.86	11.07
HIP-Cl(5)-OH	466	0.476	0.243	4.089	1.145	2.20/1.61	28.19
HIP-FDA(3)-Cl-OH	765	0.811	0.471	4.238	1.085	2.60/1.70	21.38
HIP-EDC-Cl-OH	1480	1.903	0.887	5.144	1.080	2.82/2.26	15.50

[a] BET surface area.
[b] Total pore volume.
[c] Microporous volume estimated by the DR method method.
[d] Average pore size for total pores.
[e] Most probable aperture of micropores volume.
[f] CO_2 uptakes at 273 K and 298 K (1 bar).

Table S2 Elemental analysis of HIPs.

Sample	C%	H%	S%	N%	IL Content (mmol g^{-1})
HIP-Cl(1)-OH	75.51	5.892	0.054	2.57	0.918
HIP-Cl(3)-CH_3	62.32	5.665	0.321	3.84	1.371
HIP-Cl(3)-COOH	71.48	4.710	0.135	2.00	0.714
HIP-Cl(3)-OH	66.46	5.549	0.112	2.72	0.971
HIP-Cl(3)-OH-Re[a]	67.40	5.392	0.527	2.67	0.954
HIP-Br(3)-OH	64.58	4.926	0.036	2.62	0.935
HIP-Cl(5)-CH_3	62.76	5.699	0.528	3.44	1.229
HIP-Cl(5)-COOH	62.45	4.573	0.086	1.23	0.439
HIP-Cl(5)-OH	64.84	5.234	0.062	2.65	0.946
HIP-FDA(3)-Cl-OH	71.21	5.759	0.236	2.37	0.846
HIP-EDC-Cl-OH	79.20	4.510	0.206	0.98	0.350

[a] Reused after six runs.

Table S3 Activity of meatl-free porous ionic polymers in the cycloaddition of CO_2 with styrene oxide.

Catalyst	t (h)	Tem (K)	CO_2 (MPa)	Co-catalyst	Yield (%)	Homogeneous/ Heterogeneous	Ref.
catalyst **4**	24	373	0.1	None	80	Homogeneous	1
SiO_2-His	10	403	0.5	None	99	Heterogeneous	2
Al-PDC	20	373	0.1	None	98	Hemogeneous	3
catalyst **1**	24	373	0.1	None	99	Heterogeneous	4
lignin	10	393	1	KI	96	Heterogeneous	5
phenolated lignin nanoparticles	24	333	0.1	TBAI	76±4	Heterogeneous	6
LS-DIL-G3	5	263	1	TBAB	94	Heterogeneous	7
IC2HCP-5b	32	393	3 MPa (15% CO_2+85 % N_2)	None	87	Heterogeneous	8
HP-[BZPhIm]Cl-DCX-1	24	393	0.1	None	91	Heterogeneous	9
IHCP-OH(1)	2	408	3	None	94	Heterogeneous	10
HPILs-Cl-2	9	343	0.1	TBAB	88	Heterogeneous	11
HIP-Br-2	120	293	0.1	$ZnBr_2$	93	Heterogeneous	12
Py-HCP-Br	8	393	2	None	89	Heterogeneous	13
POM3-IM	12	393	1	None	89	Heterogeneous	14
COP-114-(CH_2NMe^{3+})maxCl$^-$	24	373	0.1	None	96	Heterogeneous	15
[HCP-CH_2-Im][Cl]-1	5	413	0.1	None	99	Heterogeneous	16
HIP-Cl(3)-OH	5	413	0.1	None	99	Heterogeneous	This worik
HIP-Cl(3)-OH	8	393	0.1	None	98	Heterogeneous	This worik
HIP-Cl(3)-OH	20	373	0.1	None	98	Heterogeneous	This worik

Supplementary References

1. W. Natongchai, J. A. Luque-Urrutia, C. Phungpanya, M. Sola, V. DElia, A. Poater, H. Zipse, *Org. Chem. Front*, 2021, **8**, 613–627.

2. A. Z. Hajipour, Y. Heidari, G. Kozehgary, *Synlett*, 2016, **27**, 929–933

3. A. Mitra, T. Biswas, S. Ghosh, G. Tudu, K. S. Paliwal, S. Ghosh, V. Mahalingam, *Sustainable Energy Fuels*, 2022, **6**, 420-429.

4. S. Subramanian, J. Park, J. Byun, Y. Jung, C. T. Yavuz, *ACS Appl. Mater. Interfaces*., 2018, **10**, 9478–9484.

5. L. Guo, R. Dou, Y. Wu, R. Zhang, L. Wang, Y. Wang, Z. Gong, J. Chen, X. Wu, *ACS Sustainable Chem. Eng*., 2019, **7**, 16585−16594.

6. W. Jaroonwatana, T. Theerathanagorn, M. Theerasilp, S. D. Gobbo, D. Yiamsawas, V. Delia, D. Crespy, *Sustainable Energy Fuels*, 2021, **5**, 5431–5444.

7. S. Lai, J. Gao, H. Zhang, L. Chen, X. Xiong, *J. CO_2 Util*., 2020, **38**, 148–157.

8. W. L. Zhang, F. P. Ma, L. Ma, Y. Zhou, J. Wang, *ChemSusChem*, 2020, **13**, 341–350.

9. H. Song, Y. Wang, Y. Liu, L. Chen, B. Feng, X. Jin, Y. Zhou, T. Huang, *ACS Sustainable Chem. Eng*., 2021, **9**, 2115−2128.

10. D. G. Jia, L. Ma. Y, Wang. W. L. Zhang, J. Li, Y. Zhou, J. Wang, *Chem. Eng. J*., 2020, **390**, 124652.

11. Y. F. Sang, J. H. Huang, *Chem. Eng. J*., 2020, **385**, 123973.

12. J. Li, D. G. Jia, Z. J. Guo, Y. Q. Liu, Y. N. Lyu, Y. Zhou, J. Wang, *Green Chem.*, 2017, **19**, 2675–2686.

13. C. Liu, L. Shi, J. Zhang, J. Sun, *Chem. Eng. J*., 2022, **427**, 131633.

14. J. Wang, W. Sng, G. Yi, Y, Zhang, *Chem. Commun*., 2015, **51**, 12076—12079

15. D. Kim, S. Subramanian, D. Thirion, Y. D. Song, A. Jamal, M. S. Otaibi, C. T. Yavuz, *Catal. Today*., 2020, **356**, 527–534.

16. X. Liao, B. Pei, R. Ma, L. Kong, X. Gao, J. He, X. Luo, J. Lin, *Catalysts*, 2022, **12**, 62.